Supporting Information

All-Weather-Available, Continuous Steam Generation Based on the Synergistic Photo-Thermal and Electro-Thermal Conversion by MXene-Based Aerogels

Xing Zhao,‡ Li-Mei Peng,‡ Chun-Yan Tang, Jun-Hong Pu, Xiang-Jun Zha, Kai Ke, Rui-Ying Bao, Ming-Bo Yang, Wei Yang*

College of Polymer Science and Engineering, Sichuan University, State Key Laboratory of Polymer Materials Engineering, Chengdu, 610065, Sichuan, China

‡Xing Zhao and Li-Mei Peng contributed equally to this work. *Corresponding authors. Tel.: + 86 28 8546 0130; Fax: + 86 28 8546 0130

E-mail: weiyang@scu.edu.cn (W Yang)

Experimental Section

Materials: Layered ternary carbide (Ti_3AlC_2) MAX phase powder was procured from 11 Technology Co., LTD. Graphene Oxide (GO) was obtained from Hengqiu Tech. Inc. Concentrated hydrochloric acid (HCl, technical grade, 35–38%), Ethanol, and Ethylenediamine (EDA) were provided by Aladdin Biochemical Technology Co., Ltd. Lithium fluoride (LiF, 98+%) was purchased from Alfa Aesar. Polypropylene membrane (3501 coated PP) was procured from Celgard LLC, NC. All the materials were used as received.

Synthesis of MXene and GO: MXene ($Ti_3C_2T_x$) was synthesized by etching the Ti_3AlC_2 MAX phase with LiF/HCl solution. Typically, 1 g LiF was dissolved in 20 ml 9M HCl in a Teflon container under magnetic stirring for 5 minutes to ensure the dissolution of LiF. Then, 1 g Ti_3AlC_2 powder was slowly added into the LiF/HCl etching solution (in over 5 min), and the mixture reacted at 35 °C for 24 h under magnetic stirring to obtain a stable suspension. The resultant $Ti_3C_2T_x$ suspension was repeatedly washed

with deionized water and centrifuged at 3500 rpm for 5 min until pH > 5. The obtained $Ti_3C_2T_x$ powder was dried under vacuum at 60 °C overnight. The delamination of $Ti_3C_2T_x$ was conducted by sonication treatment followed by centrifugation for 1 h at 3500 rpm to obtain a homogeneous supernatant with delaminated $Ti_3C_2T_x$ (MXene). The concentration of the resultant MXene colloidal solution was determined by filtering a known volume of the solution on a polypropylene filter (Celgard 3501 coated PP) and measuring the weight of the resulting freestanding film after vacuum drying. GO colloidal suspensions with different concentrations were prepared by ultrosonication and mechanical stirring of GO powders in water for 1 h.

Preparation of Crosslinked MXene Hydrogels and Aerogels: A typical CMH with 90 wt% MXene was synthesized as following: MXene colloidal suspension (9 mL, 8 mg mL^{-1}) and appropriate amounts of GO suspension (1 mL, 8 mg mL^{-1}) were directly mixed together and then sonicated for about 20 min to obtain a homogeneous solution. Then 40 μL EDA was added into the mixture under mechanical stirring for another 20 min. It was then sealed in a Teflon vessel for hydrothermal treatment at 85 °C for 2 h for the co-gelation assembly of crosslinked MXene hydrogel. After being cooled to room temperature, the as-formed hydrogel was washed several times using DI water to remove residual EDA, and then was dialyzed in a 20 vol% ethanol solvent (anti-freezing agent) for 12 h. Then it was subjected to directional-freezing process, in which the hydrogel was put on a copper plate which was pre-cooled in liquid nitrogen. After freeze-drying, crosslinked MXene aerogel was obtained. To explore the effect of MXene content on the assembly and performance of CMAs, the MXene content was tuned by varying the mass ratio of MXene suspension with a constant total concentration of MXene and GO in the suspension (8 mg mL^{-1}). The ultimate CMA samples with 0, 10, 30, 50, 70, and 90% of MXene were denoted as GA, CMA-10%, CMA-30%, CMA-50%, CMA-70% and CMA-90%, respectively. For comparison, in the absence of EDA, the self-assembled MXene/GO aerogels were fabricated by the same procedure.

Characterization: Zeta potentials were measured with a Nano-ZS Zetasizer. SEM images were recorded using a JEOL JSM-5900LV scanning electron microscope (SEM, Japan) at an accelerating voltage of 15 kV. Energy-dispersive X-ray spectroscopy (EDX) and mapping were acquired with the

same machine. Transmission electron microscopy (TEM) images were obtained on a high-resolution transmission electron microscope (Tecnai G2 F20S-TWIN) equipped with a field emission gun operating at 200 kV. FTIR spectroscopy was obtained using a FTIR spectrometer (Nicolet 560). X-ray photoelectron spectrum (XPS) was performed on an XSAM800 X-ray Photoelectron Spectrometer (Kratos Company, UK) with the Al Kα radiation (hv =1486.6 eV). X-ray diffraction (XRD) analysis was carried out on a Japan Rigaku X-ray diffractometer (UItima Ⅳ) from 2θ angle of 5 ° to 45 ° using Cu Kα radiation (λ = 0.154056 nm) at a scanning speed of 10° min^{-1}. Raman spectra were obtained on a Labram HR spectrometer (HORIBA Jobin Yvon). The absorption performance was measured in the wavelength range of 250-1500 nm using an ultraviolet-visible near-infrared (UV-vis-NIR) spectrophotometer (UV3600, Shimadzu, Japan) equipped with an integration sphere. The integrating sphere was used to collect the scattered light for accurate measurements. Rheological measurements were performed on a stress-controlled rotational rheometer (AR2000EX, TA Instruments, USA). The electrical conductivity was measured using Van Der Pauw 4-probe technology.

Steam generation and desalination experiments: To evaluate the steam generation performance, a 200 mL beaker filled with water was placed on the electronic balance with an accuracy of 0.001 g. The steam generation experiments were performed by placing the CMAs on a piece of wood floating on the surface of water. The CMAs were irradiated by a lab-made device with a solar light simulator (CEL-HXUV300 xenon lamp, CEAULIGHT, China) and an optical filter for the standard AM 1.5 solar spectrum under an ambient temperature of ~25 °C. The power density of the solar light irradiation was determined by an accessional detector (CEL-NP2000 optical power meter, CEAULIGHT, China). The temperature was measured with an IR thermal camera (Fluke). The mass change of water after different time periods was recorded under different total energy input. The seawater desalination performance was evaluated by using a simulated all-in-one device manually fabricated with lab-available materials. The standard seawater was employed and the concentrations of Na^+, K^+, Ca^{2+} and Mg^{2+} ions before and after desalination were measured by inductively coupled optical emission spectroscopy (ICP-OES).

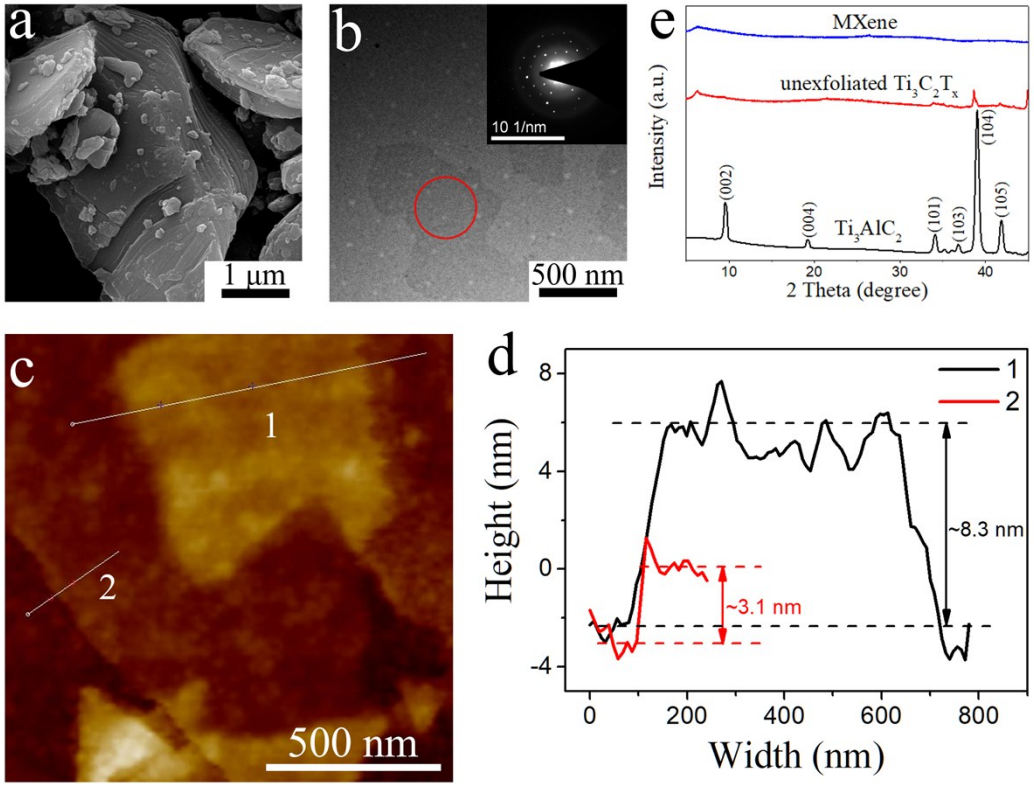

Fig. S1 (a) SEM image of Ti_3AlC_2. (b) TEM image of the delaminated MXene sheets with SAED pattern (inset), the selected area is marked with a red circle. (c) The AFM image of delaminated MXene sheets. (d) The corresponding height profiles for MXene sheets shown in the AFM image. (e) XRD patterns of Ti_3AlC_2, unexfoliated $Ti_3C_2T_x$, and delaminated $Ti_3C_2T_x$ (MXene).

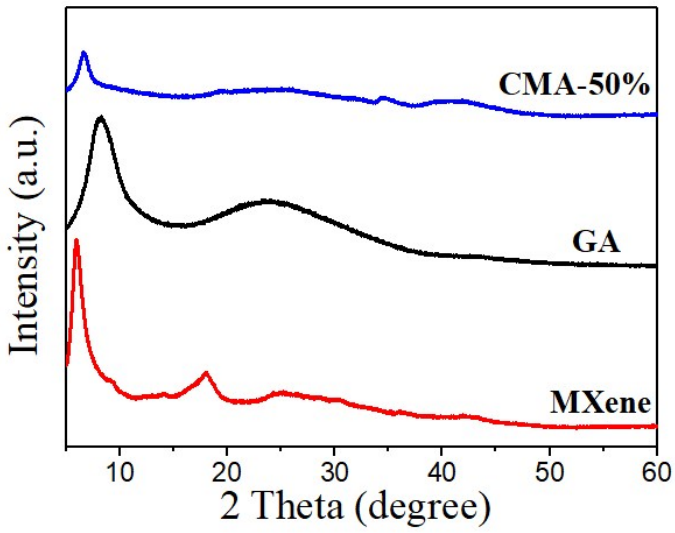

Fig. S2 XRD patterns of MXene, GA and CMA-50%.

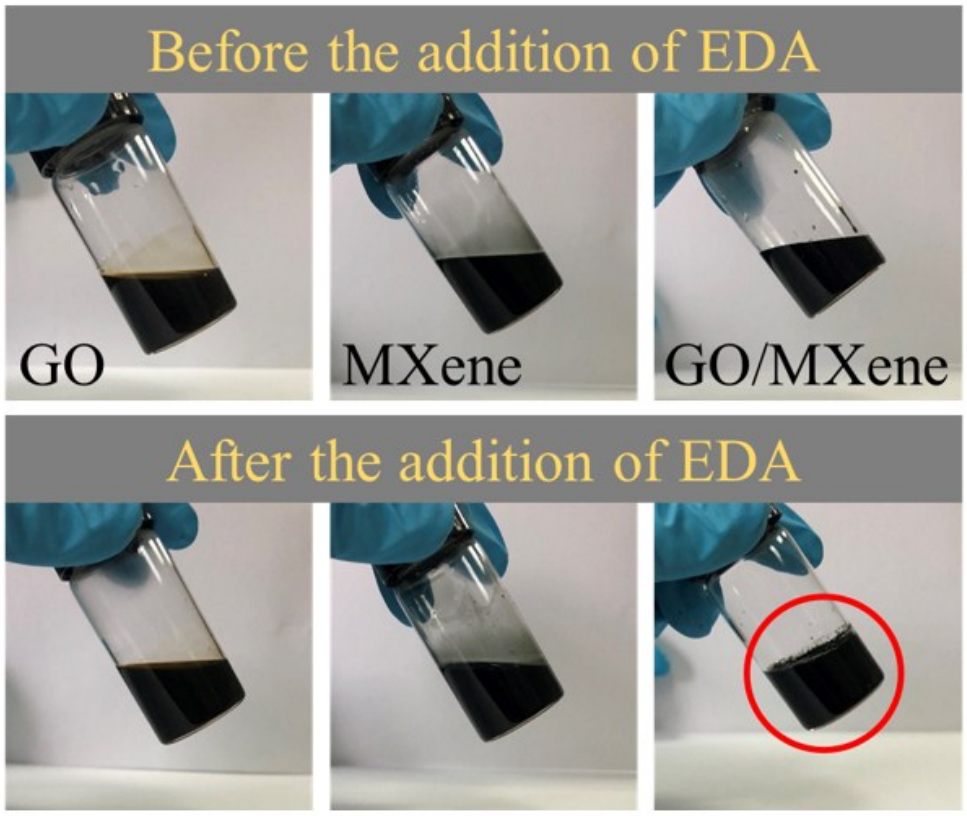

Fig. S3 Digital photographs of GO, MXene, and GO/MXene suspensions before and after the addition of EDA.

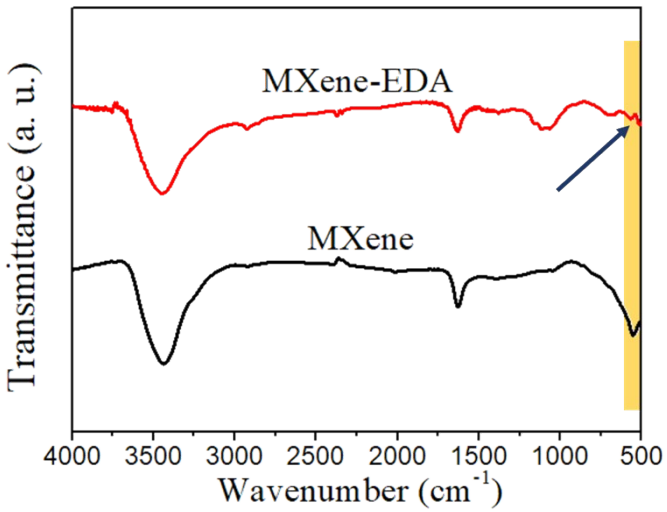

Fig. S4 FTIR spectra of pure MXene and MXene-EDA composite.

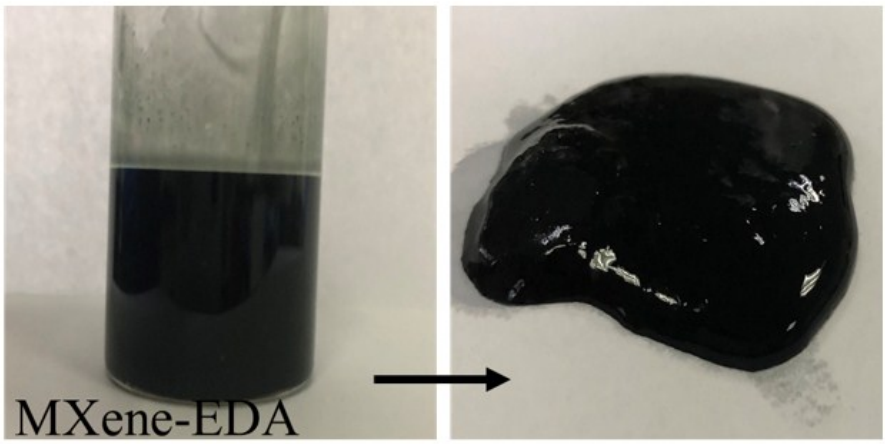

Fig. S5 Optical photographs of MXene-EDA suspensions before and after reaction at 80 °C for 2 h.

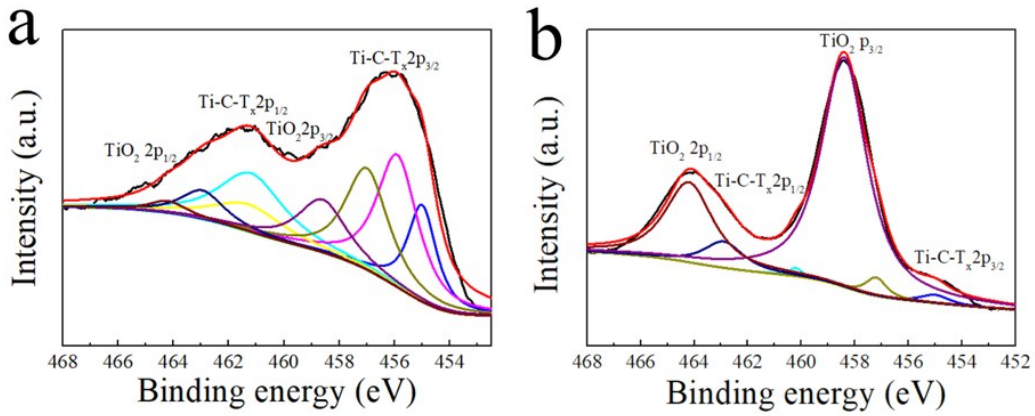

Fig. S6 High resolution X-ray photoelectron spectrometer (XPS) patterns of the Ti 2p of (a) MXene and (b) CMA-50%.

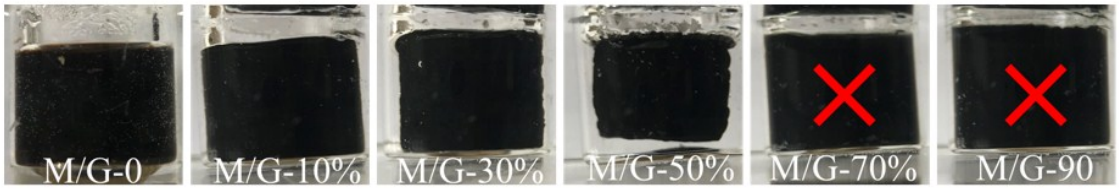

Fig. S7 Optical photographs of the hydrogels prepared with different content MXene free of EDA.

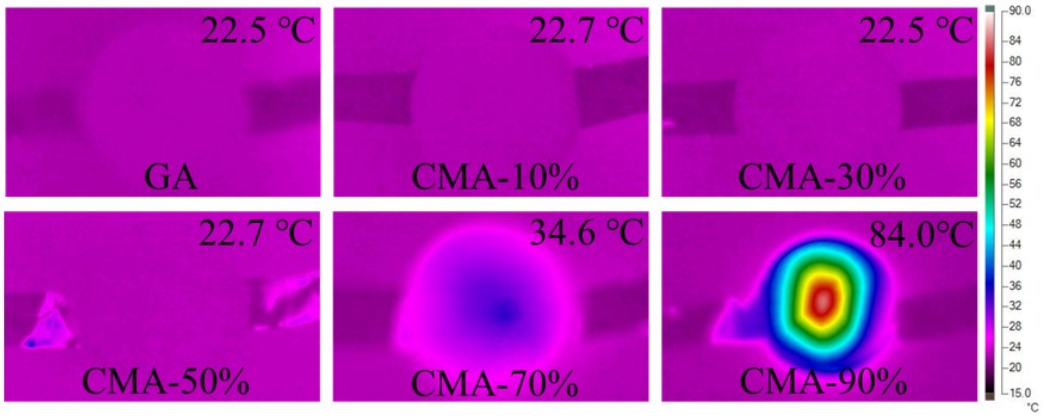

Fig. S8 IR thermal images for different CMA with different contents of MXene under applied voltage of 5V.

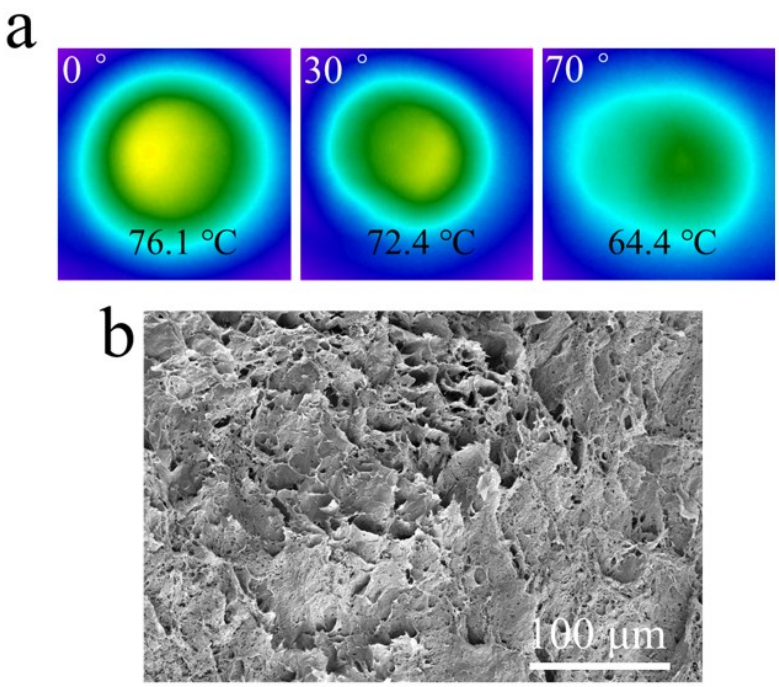

Fig. S9 (a) IR thermal images of M/G aerogel free of EDA at varied incident angles (0°, 30°, and 70°) after reaching temperature stable state under solar illumination of 1 kW m^{-2}. (b) Top-view SEM image of M/G aerogel without EDA.

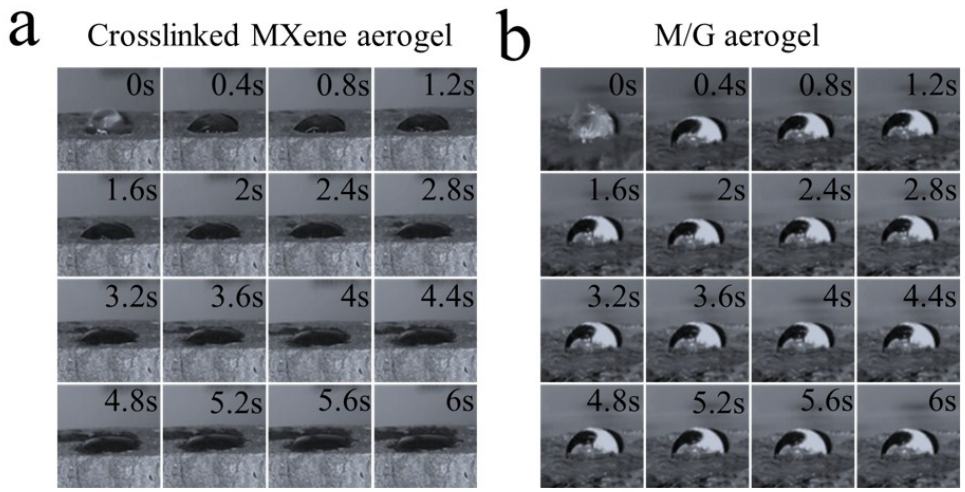

Fig. S10 Camera photos of droplet impregnation process on the surface of (a) CMA, and (b) M/G aerogel without EDA.

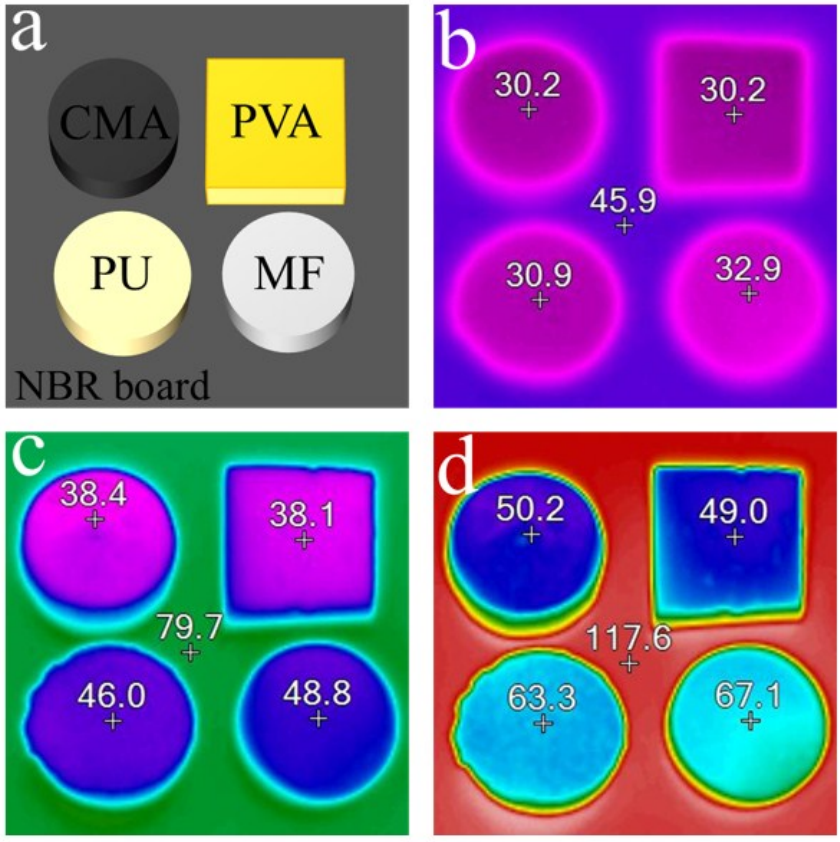

Fig. S11 (a) Scheme of CMA, PVA, PU, and MF placed on the NBR board. IR thermal images of the samples captured at 5 min when the temperature of the heating platform was set to (b) 50 °C, (c) 100 °C, and (d) 140 °C.

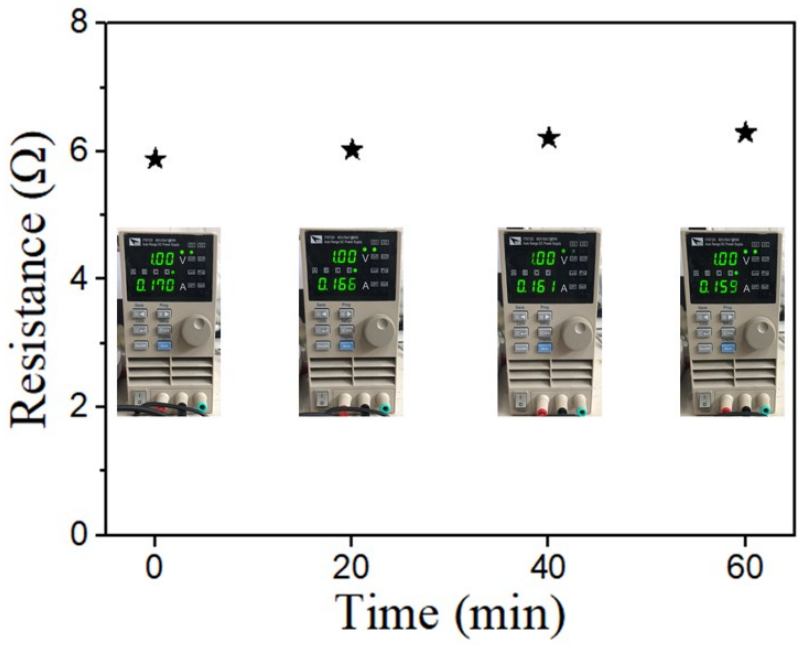

Fig. S12 (a) Resistance change of CMA during water evaporation process. Inset: Optical photographs showing the voltage and current during electricity-driven steam generation process.

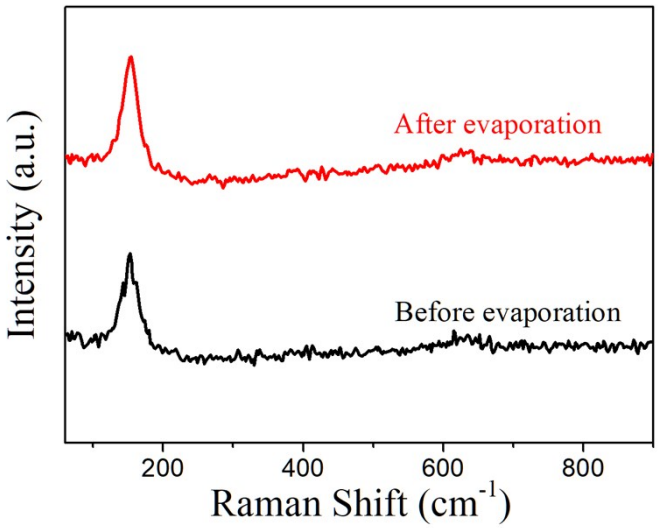

Fig. S13 high-resolution Raman spectra of CMA aerogel before and after evaporation.